Vertical excitation energies of linear cyanine dyes by spin-flip time-dependent density functional theory

AUTHOR(S):

Minezawa, Noriyuki

CITATION:

Minezawa, Noriyuki. Vertical excitation energies of linear cyanine dyes by spin-flip time-dependent density functional theory. Chemical Physics Letters 2015, 622: 115-119

ISSUE DATE:

2015-02

URL:

http://hdl.handle.net/2433/196075

Vertical excitation energies of linear cyanine dyes by spin-flip time-dependent density functional theory

Noriyuki Minezawa

Fukui Institute for Fundamental Chemistry, Kyoto University,

Sakyo-ku, Kyoto 606-8103, Japan

E-mail: minezawa@fukui.kyoto-u.ac.jp

Abstract

Vertical excitation energies of linear cyanine dyes are examined using the spin-flip time-dependent density functional theory. The Hartree-Fock exchange (HFX) plays an essential role in predicting the absorption spectra, and the best values are obtained by the combination of collinear approximation and hybrid functionals with ~50 % HFX. The non-collinear approach with pure density functionals underestimates the excitation energy severely. The significant error is due to low excitation energy from the reference triplet to first excited singlet state. The excitation energy decomposition gives small orbital energy difference term and large negative non-collinear kernel.

1. Introduction

Accurate prediction of excitation energies is of critical importance not only for designing new molecular materials but for analyzing the photochemical processes after light absorption. Computing the absorption energies of linear cyanine dyes (Figure 1), which forms π-conjugation along the chain, is challenging to theoretical methods. The observation is surprising because the lowest excited-state is described as the excitation from the highest occupied molecular orbital (HOMO) to the lowest unoccupied molecular orbital (LUMO). Several benchmark studies have been reported using various methodologies including multi-reference perturbation theory, many-body perturbation theory, coupled cluster, diffusion Monte Carlo (DMC), and density functional theory [1-6].

The linear-response time-dependent density functional theory (LR-TDDFT) [7] is a promising approach to simulate the excitation energies for large molecules with modest computational cost. A large number of benchmark studies have been reported to investigate the performance of LR-TDDFT and to propose new density functionals [8]. The previous studies on linear cyanine dyes show the LR-TDDFT method overestimates the excitation energy [2-4]. Grimme and Neese found that the double hybrid functional yields the better

result [9]. These authors argued the difference of electronic correlation between the ground and excited states is partially accounted for by the correlation energy of the second-order Møller-Plesset perturbation theory (MP2) and the configuration interaction singles with doubles correction. The notorious charge-transfer problem that is inherent in the LR-TDDFT is not severe for these molecules; the range-separated functional does not improve the results [10].

This Letter reports the computational study on the excitation energy of linear cyanine dyes by using the spin-flip TDDFT (SF-TDDFT) [11-19]. This approach has been successfully applied to describe the conical intersections of ethylene, butadiene, and the model chromophore of protonated Schiff base retinal [20-23]. Thus, it is interesting to examine the accuracy by applying the SF-TDDFT to linear cyanine dyes. Furthermore, one expects that the SF-TDDFT can take into account the correlation energy contribution of LUMO explicitly because the reference triplet state is $(\mathrm{HOMO})^1(\mathrm{LUMO})^1$. Very recently, Filatov and Huix-Rotllant have investigated linear cyanine dyes using the ensemble DFT, LR-TDDFT, SF-TDDFT and ΔSCF (self-consistent field) methods [24]. In the SF-TDDFT computation, these authors employed exclusively the hybrid functional with ~50 %

Hartree-Fock exchange (HFX) in conjunction with the collinear approximation. This work introduces various functionals including local density approximation (LDA), semi-local generalized gradient approximation (GGA), hybrid GGA, and meta-GGA functionals. In addition, a comparison is made between the collinear and non-collinear approaches implemented in the program package GAMESS [25,26]. The latter formulation is general and applicable to any functionals while the collinear approximation allows only the hybrid functionals.

2. Method

2.1. Non-collinear SF-TDDFT method

In this work, the non-collinear SF-TDDFT method [12-19] is developed within the Tamm-Dancoff approximation. The SF-TDDFT employs the triplet state with two unpaired alpha electrons as the reference, and the response states are described by alpha-to-beta spin-flip excitations. The transition amplitude $\mathbf{X}$ and excitation energy Ω are obtained by solving the Hermitian matrix equation:

$$\mathbf{AX} = \Omega\mathbf{X} \tag{1}$$

The coupling matrix $\mathbf{A}$ is

$$A_{i\bar{a},j\bar{b}} = (\varepsilon_{\bar{a}} - \varepsilon_i)\delta_{ij}\delta_{\bar{a}\bar{b}} + f^{\mathrm{ncol}}_{i\bar{a},j\bar{b}} - c_x(ij|\bar{a}\bar{b}) \tag{2}$$

As usual, $i, j, \cdots$ label the occupied orbitals and $a, b, \cdots$ the virtual orbitals. The bar symbol denotes the beta spin. ε is the orbital energy, and c_x is the mixing weight of HFX. Mulliken notation is adopted for the two-electron integral. The second term of Eq. (2) is the non-collinear kernel:

$$f^{\mathrm{ncol}}_{i\bar{a},j\bar{b}} = \int d\mathbf{r} \frac{\frac{\delta E^{\mathrm{xc}}}{\delta n_\alpha(\mathbf{r})} - \frac{\delta E^{\mathrm{xc}}}{\delta n_\beta(\mathbf{r})}}{n_\alpha(\mathbf{r}) - n_\beta(\mathbf{r})} \psi_i(\mathbf{r})\psi_j(\mathbf{r})\bar{\psi}_a(\mathbf{r})\bar{\psi}_b(\mathbf{r}) \tag{3}$$

The numerator is the difference between the exchange potential, and the denominator is the spin density of the reference state, i.e., the triplet state with two unpaired alpha electrons.

Shao et al. [11] have developed the collinear approximation by neglecting the non-collinear kernel ($\mathbf{f}^{\mathrm{ncol}}$). In this case, only the HFX term contributes the off-diagonal elements of the coupling matrix. Thus, one must employ the functionals with a fraction c_x of HFX. Otherwise, the coupling matrix is diagonal and gives the orbital energy difference as the excitation energy.

For the non-collinear calculations, three approaches are considered here. The first method (NCOL0) computes Eq. (3) rigorously. Using the partial integration, Li and Liu [16] evaluate this term as the second functional derivatives ($\delta^2 E^{\mathrm{xc}} / \delta n \delta n$) and the second derivatives of electron density ($\nabla\nabla n$). This formulation yields nearly zero excitation energy for the response ($M_S = 0$) triplet states. The drawback is severe numerical instability as pointed out in Ref. [16]. The second approach (NCOL1) can eliminate the instability entirely by setting the terms stemming from the density derivative (∇n) and kinetic energy density (τ) to be zero

$$\frac{\frac{\delta E^{\mathrm{xc}}}{\delta n_\alpha(\mathbf{r})} - \frac{\delta E^{\mathrm{xc}}}{\delta n_\beta(\mathbf{r})}}{n_\alpha(\mathbf{r}) - n_\beta(\mathbf{r})} \rightarrow \left[\frac{\frac{\partial E^{\mathrm{xc}}}{\partial n_\alpha(\mathbf{r})} - \frac{\partial E^{\mathrm{xc}}}{\partial n_\beta(\mathbf{r})}}{n_\alpha(\mathbf{r}) - n_\beta(\mathbf{r})} \right]_{\nabla n = \tau = 0} \tag{4}$$

Note the change from the functional derivative to the density derivative. Li and Liu call this approximation ALDA0 and show that this replacement can provide numerically stable results even for GGA functionals [16]. The last approach (NCOL2) replaces the functional derivative by the derivative with respect to explicit density but keeps the density derivative and kinetic energy density

$$\frac{\frac{\delta E^{\mathrm{xc}}}{\delta n_\alpha(\mathbf{r})} - \frac{\delta E^{\mathrm{xc}}}{\delta n_\beta(\mathbf{r})}}{n_\alpha(\mathbf{r}) - n_\beta(\mathbf{r})} \rightarrow \frac{\frac{\partial E^{\mathrm{xc}}}{\partial n_\alpha(\mathbf{r})} - \frac{\partial E^{\mathrm{xc}}}{\partial n_\beta(\mathbf{r})}}{n_\alpha(\mathbf{r}) - n_\beta(\mathbf{r})} \tag{5}$$

In contrast to NCOL1, this approximation encounters numerical instability when n_α

approaches n_β. The numerator does not always converge to zero due to the density derivative and the kinetic energy density.

2.2. SF-TDDFT excitation energies

The SF-TDDFT excitation energies are calculated using the three approaches [18,19]. The first method (SF1) computes the energy as follows:

$$\begin{aligned}\Delta E^{\mathrm{SF1}} &= E^{\mathrm{SF}}(\mathrm{S}_1) - E^{\mathrm{SF}}(\mathrm{S}_0) \\ &= \Omega(\mathrm{S}_1 \,|\, \mathrm{T}_1) - \Omega(\mathrm{S}_0 \,|\, \mathrm{T}_1)\end{aligned} \tag{6}$$

where $\Omega(\mathrm{S}_1 \,|\, \mathrm{T}_1)$ denotes the excitation energy from the reference triplet T_1 to singlet S_1 state. Similary, $\Omega(\mathrm{S}_0 \,|\, \mathrm{T}_1)$ is the transition energy from the reference T_1 to ground state S_0. Both $\Omega(\mathrm{S}_0 \,|\, \mathrm{T}_1)$ and $\Omega(\mathrm{S}_1 \,|\, \mathrm{T}_1)$ are obtained by the standard SF-TDDFT calculation. The SF1 method is simple and yields the excitation energy by a single energy calculation. Moreover, the S_0 and S_1 states can be treated on an equal footing.

The second method (NSF2) [18,19] uses the ground-state Kohn-Sham (KS) DFT energy instead of $E^{\mathrm{SF}}(\mathrm{S}_0)$,

$$\Delta E^{\mathrm{NSF2}} = E^{\mathrm{SF}}(\mathrm{S}_1) - E^{\mathrm{KS}}(\mathrm{S}_0) \tag{7}$$

The NSF2 method is intended to correct the closed-shell ground state on the assumption that the KS-DFT energy gap is more accurate than the SF-TDDFT $\Omega(\mathrm{S}_0 \mid \mathrm{T}_1)$. Equation (7), however, may introduce some bias due to two different methods employed.

The last method (SF2) [18,19] uses Yamaguchi's spin projection formula [27] to eliminate the spin contamination of the S_1 state,

$$\Delta E^{\mathrm{SF2}} = \Delta E^{\mathrm{NSF2}} - \left[\Omega(\mathrm{S}_1 \mid \mathrm{T}_1) - \frac{2\,\Omega(\mathrm{S}_1 \mid \mathrm{T}_1)}{\left\langle S^2 \right\rangle_{\mathrm{T}_1} - \left\langle S^2 \right\rangle_{\mathrm{S}_1}} \right] \tag{8}$$

where $\langle S^2 \rangle$ is the spin expectation value of $\hat{S}^2$ for the unrestricted KS T_1 state or the spin-flipped S_1 state.

2.3. Computational details

The developed codes were interfaced with the program package GAMESS [25,26]. Geometries at the MP2/cc-pVQZ level were taken from Ref. [4]. The linear cyanine molecules have C_{2v} symmetry, and the excitation from the ground (A_1) to the lowest (B_2)

singlet state was considered. Unrestricted KS-DFT was used to describe the reference B_2 triplet state, in which two singly occupied π orbitals have b_1 and a_2 symmetries. The functionals examined in this work are LDA (SVWN [28,29]), semi-local and hybrid GGA (BLYP [30,31], B3LYP [32-34], BHHLYP [30,31], PBE [35,36], PBE0 [35-37], PBE50 [17]), range-separated CAMB3LYP [38], and meta-GGA (M06 [39], M06-2X [39], M06-HF [40]). The basis set employed was TZVP [41,42], and the deviation of excitation energy is 0.02 eV compared to the largest basis set (see Table S1 in the Supplementary material). The numerical integration was performed using 96 radial points and 590 Lebedev's angular grid. The collinear approach requires the non-zero HFX, and thus pure density functionals are not applicable. Also, the NCOL0 approach is not available for meta-GGA because it is difficult to develop the rigorous integration of kinetic energy density.

3. Results and Discussion

Tables in the text are constructed using the data presented in Tables S2-S5 (see the Supplementary material), which summarize the total energies of the A_1 and B_2 states as

well as the spin expectation values. Since the latter values are around 0 and 2 for the singlet and triplet states, the spin-contamination is less severe for cyanine dye molecules.

3.1. Linear-response TDDFT method

Table 1 summarizes the excitation energies obtained by the conventional LR-TDDFT with various functionals. The mean signed error (MSE) is estimated using the DMC [2] values as a reference. For clarity, bold font highlights the mean absolute error that is less than 0.3 eV. Similar MSE values indicate a weak functional dependence for the present molecules. As observed in the previous studies [2-4], all functionals give positive MSE values and overestimate the excitation energies compared to the DMC. The LR-TDDFT excitation energy weakly depends on the chain length compared to the DMC result, and the slope of excitation energy is less steep. As a result, the deviation is largest for CN11. The best functional is M06-HF (the MSE of 0.14 eV) followed by M06-2X (0.29 eV). Therefore, the LR-TDDFT is a method of choice to simulate the excitation energies of cyanine dyes.

3.2. Collinear SF-TDDFT method

Table 2 shows the absorption energies obtained by the collinear SF-TDDFT with the SF1 method. Note the collinear approximation is only applicable to hybrid functionals. The collinear SF-TDDFT also gives satisfactory results. Adding more weight of HFX gives rise to the increase of MSE: PBE0 (−0.25 eV) to PBE50 (0.23 eV), B3LYP (−0.38 eV) to BHHLYP (0.20 eV), and M06 (−0.32 eV) to M06-2X (0.12 eV) to M06-HF (0.41 eV). Similar chain length dependence is observed as in the case of LR-TDDFT. The decrease in the excitation energy is moderate compared to the DMC. For the longest CN11, the functionals with negative MSEs yield the energy that is comparable to the DMC. In contrast, the deviation is large for the functionals with positive MSEs. Overall, the functionals containing about 50 % HFX outperform the others. The best functional is M06-2X (0.12 eV) followed by BHHLYP (0.20 eV) and PBE50 (0.23 eV).

It is interesting to compare the results with those by the LR-TDDFT in Table 1. For almost all functionals, the MSE of SF-TDDFT is smaller than that of LR-TDDFT. The exception is M06-HF: the SF-TDDFT MSE overshoots the LR-TDDFT one by 0.27 eV. Interestingly, M06-HF, which works best for the LR-TDDFT, becomes worst in the collinear SF-TDDFT.

3.3 Noncollinear SF-TDDFT method

Table 3 summarizes the vertical transition energies obtained by the non-collinear SF-TDDFT. As presented in Sec. 2.1, the three variants are considered in this work. A broader class of functionals is available at the non-collinear level. Note the NCOL0 approach is not applicable to meta-GGA. Apparently, the LDA functional (SVWN) gives the identical results. The error introduced by the approximation, Eqs. (4) and (5), is small: the MSEs for the NCOL1 and NCOL2 increase slightly (~0.1 eV) compared to NCOL0. For the meta-GGA, however, the NCOL1 and NCOL2 results differ significantly (~0.4 eV). As in the case of collinear approach, adding the HFX increases the MSE: BLYP series (−0.98, −0.51, and 0.12 eV), PBE (−0.97, −0.39, and 0.13 eV), and M06 (−0.84, −0.04, and 1.40 eV).

The introduction of the non-collinear kernel does not seem to improve the excitation energies. In particular, this holds true for the hybrid functionals that already give reasonable MSE values at the collinear approximation level. The functional whose MSE becomes

close to zero is only a few: BHHLYP, M06-2X, and PBE50. The LDA (SVWN) and semi-local GGA (BLYP and PBE) functionals underestimates the excitation energies severely (the MSE of −1.0 eV), and none of these functionals is acceptable.

3.4. Excitation energy decomposition

Tables S6 and S7 in the Supplementary material show the NSF2 and SF2 excitation energies. The former method cures the inaccuracy of the gap between the lowest singlet and triplet states while the latter alleviates the spin-contamination for the relevant electronic states [18,19]. These methods improve the results of collinear B3LYP and M06 only. As shown in Tables 2, S6, and S7, the MSE of B3LYP changes from −0.38 eV (SF1) to −0.21 eV (NSF2 and SF2) and that of M06 from −0.32 eV to −0.22 eV. No substantial improvement for other functionals indicates that the SF-TDDFT reproduces the energy gap and that the spin-contamination is not severe (see Tables S2-S5).

It is interesting to see why LDA and semi-local GGA functionals underestimate the excitation energies severely. To this end, the excitation energies $\Omega(S_0 \mid T_1)$ and $\Omega(S_1 \mid T_1)$

are decomposed into a few terms as in Ref. [17].

$$\begin{aligned}\Omega &= \mathbf{X}^{\dagger}\mathbf{A}\mathbf{X} \\ &= \sum_{\bar{a},\bar{b}}^{\text{virt}}\sum_{i,j}^{\text{occ}} X_{i\bar{a}} X_{j\bar{b}} \left[(\varepsilon_{\bar{a}} - \varepsilon_i)\delta_{\bar{a}\bar{b}}\delta_{ij} + f_{ij\bar{a}\bar{b}}^{\text{ncol}} - c_x(ij \mid \bar{a}\bar{b}) \right] \\ &\equiv \Omega(\text{dia}) + \Omega(\text{XC2}) + \Omega(\text{K2})\end{aligned} \tag{9}$$

The first term estimates the contribution from the diagonal element of the coupling matrix. The second and third terms are the excitation energy due to the non-collinear kernel and the HFX integral, respectively. Table 4 shows the results of CN5 for some selected functionals. The excitation energy $\Omega(S_1 \mid T_1)$ has stronger functional dependence than the energy $\Omega(S_0 \mid T_1)$. Thus, the accuracy of $\Omega(S_1 \mid T_1)$ is a key to improving the excitation energy values. For the BHHLYP and M06-2X functionals, the K2 term compensates large diagonal contribution and the presence of XC2 determines the difference in the transition energy. For LDA and semi-local GGA functionals, the energy $\Omega(S_1 \mid T_1)$ reflects too small diagonal part (~1 eV) and large negative non-collinear kernel (~−0.5 eV). Therefore, the description of the reference triplet state is problematic for these functionals.

It is interesting to compare the present results to those reported in the previous studies. Using the LR-TDDFT and ΔSCF methods, Zhekova et al. [6] argued that a fraction HFX of ~50 % affords good estimates of both the singlet and triplet states and the singlet-triplet

gaps. These authors shows that the LR-TDDFT triplet excitation energies are only moderately dependent on density functionals and that too low triplet excitation energy gives rise to large singlet-triplet gap and too high singlet excitation energies. As shown in Table 5, the SF-TDDFT transition energy $\Omega(S_0|T_1)$, which corresponds to the minus of triplet excitation in the LR-TDDFT, has also weak dependence on density functionals. However, the SF-TDDFT singlet-triplet gap, $\Omega(S_1|T_1)$, seems to be too large and small for hybrid and pure functionals, respectively.

In summary, the SF-TDDFT calculations show that the HFX plays a dominant role in predicting the absorption energies of linear cyanine dyes whether or not the non-collinear kernel is introduced. The collinear SF-TDDFT using the functionals with ~50 % HFX gives the best MSE and is highly recommended. The non-collinear approximation with pure functionals is not an attractive choice in this work. This formulation increases the computational cost due to the evaluation of the kernel. Furthermore, the NCOL0 and NCOL2 are numerically instable and suffer from spurious roots during the excitation energy calculation although one can eliminate these shortcomings using the NCOL1 (ALDA0) option. The analytic energy gradient is not available, and it is difficult to explore

excited-state potential energy surfaces.

4. Summary

In the present work, vertical excitation energies of linear cyanine dyes are examined using the SF-TDDFT method. The excitation energy is calculated using both the collinear and non-collinear approaches, and three variants for the latter are introduced. The calculated results show the Hartree-Fock exchange (HFX) plays an essential role in predicting the absorption spectra. The best values are obtained by the collinear approximation using the hybrid functionals with ~50 % HFX (M06-2X, BHHLYP, and PBE50), and these functionals are highly recommended. Contrastively, the non-collinear approach with pure functionals underestimates the excitation energy severely, and none of the LDA and semi-local functionals gives acceptable results (MSE of −1.0 eV). The significant error is due to low excitation energy from the reference triplet to first excited singlet state. The excitation-energy decomposition gives small orbital energy difference term and large negative non-collinear kernel.

Figure 1. Molecular structure of cyanine dyes.

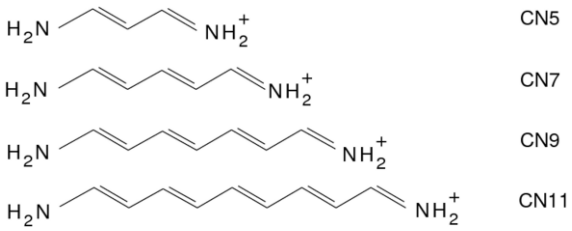

Table 1

Excitation energies by conventional linear-response TDDFT.[a] Unit: eV.

Functional	CN5	CN7	CN9	CN11	MSE[a]
BLYP	5.28	4.13	3.46	3.00	0.32
B3LYP	5.35	4.19	3.50	3.03	0.38
BHHLYP	5.49	4.28	3.57	3.08	0.46
CAMB3LYP	5.33	4.16	3.46	2.99	0.34
M06	5.30	4.14	3.46	2.99	0.33
M06-2X	5.26	4.10	3.41	2.94	**0.29**
M06-HF	5.13	3.95	3.26	2.78	**0.14**
PBE	5.31	4.15	3.47	3.01	0.34
PBE0	5.40	4.22	3.52	3.05	0.41
PBE50	5.51	4.30	3.57	3.09	0.47
SVWN	5.30	4.15	3.47	3.01	0.34

[a]Reference is the DMC excitation energies: 5.03, 3.83, 3.09, and 2.62 eV [2].

Table 2

Excitation energies by collinear SF-TDDFT with the SF1 method.[a] Unit: eV.

Functional	CN5	CN7	CN9	CN11	MSE[a]
B3LYP	4.60	3.41	2.74	2.31	−0.38
BHHLYP	5.18	4.00	3.32	2.87	**0.20**
CAMB3LYP	5.21	4.11	3.46	3.04	0.31
M06	4.64	3.47	2.81	2.38	−0.32
M06-2X	5.06	3.93	3.26	2.82	**0.12**
M06-HF	5.27	4.22	3.57	3.15	0.41
PBE0	4.74	3.54	2.86	2.42	**−0.25**
PBE50	5.22	4.03	3.34	2.88	**0.23**

[a]Reference is the DMC excitation energies: 5.03, 3.83, 3.09, and 2.62 eV [2].

Table 3

Excitation energies by non-collinear SF-TDDFT with the SF1 method.[a] Unit: eV.

Functional	CN5	CN7	CN9	CN11	MSE[b]
BLYP	3.85	2.73	2.12	1.74	−1.03
	3.93	2.79	2.16	1.77	−0.98
	3.95	2.80	2.17	1.78	−0.97
B3LYP	4.35	3.23	2.58	2.18	−0.56
	4.43	3.27	2.62	2.21	−0.51
	4.45	3.29	2.63	2.22	−0.50
BHHLYP	5.15	3.87	3.19	2.76	**0.10**
	5.09	3.92	3.24	2.80	**0.12**
	5.13	3.94	3.27	2.82	**0.15**
CAMB3LYP	4.96	3.89	3.27	2.86	**0.11**
	5.00	3.94	3.31	2.90	**0.15**
	5.04	3.96	3.33	2.92	**0.17**

M06			N/A		
	3.98	2.94	2.34	1.96	−0.84
	4.43	2.99	2.60	2.17	−0.59
M06-2X			N/A		
	4.87	3.76	3.11	2.68	**−0.04**
	5.26	4.19	3.49	3.08	0.36
M06-HF			N/A		
	6.47	5.22	4.49	4.00	1.40
	6.25	5.49	4.80	4.62	1.65
PBE	3.85	2.75	2.14	1.77	−1.01
	3.95	2.80	2.17	1.78	−0.97
	3.92	2.78	2.16	1.76	−0.99
PBE0	4.50	3.36	2.68	2.26	−0.44
	4.56	3.40	2.74	2.32	−0.39
	4.52	3.38	2.73	2.30	−0.41
PBE50	5.00	3.88	3.20	2.76	**0.07**

	5.10	3.94	3.25	2.81	**0.13**
	5.05	3.91	3.23	2.78	**0.10**
SVWN	3.95	2.80	2.17	1.77	−0.97
	3.95	2.80	2.17	1.77	−0.97
	3.95	2.80	2.17	1.77	−0.97

[a]Each functional has three lines: NCOL0 (top), NCOL1 (middle), and NCOL2 (bottom).

[b]Reference is the DMC excitation energies: 5.03, 3.83, 3.09, and 2.62 eV [2].

Table 4

Excitation energy decomposition of CN5 for selected functionals.[a] Unit: eV.

Functional		Ω(dia)	Ω(K2)	Ω(XC2)	Total
BHHLYP	COL	1.28	−4.25	0.00	−2.96
		6.60	−4.38	0.00	2.22
BHHLYP	NCOL1	1.34	−4.30	−0.11	−3.07
		6.73	−4.50	−0.21	2.02
M06-2X	COL	0.98	−4.63	0.00	−3.66
		6.29	−4.89	0.00	1.40
M06-2X	NCOL1	1.11	−4.75	−0.23	−3.87
		6.57	−5.14	−0.43	1.00
SVWN	NCOL1	−3.10	0.00	−0.33	−3.43
		1.09	0.00	−0.57	0.52
BLYP	NCOL1	−2.82	0.00	−0.31	−3.13
		1.32	0.00	−0.52	0.80

[a]For each functional, the upper line shows $\Omega(S_0 \mid T_1)$ and the lower $\Omega(S_1 \mid T_1)$.

References

1. M. Schriber, V. Buß, M. P. Fülscher, Phys. Chem. Chem. Phys. 3 (2001) 3906.
2. R. Send, O. Valsson, C. Filippi, J. Chem. Theory Comput. 7 (2011) 444.
3. D. Jacquemin, Y. Zhao, R. Valero, C. Adamo, I. Ciofini, D. G. Truhlar, J. Chem. Theory Comput. 8 (2012) 1255.
4. B. Moore II, J. Autschbach, J. Chem. Theory Comput. 9 (2013) 4991.
5. P. Boulanger, D. Jacquemin, I. Duchemin, X. Blasé, J. Chem. Theory Comput. 10 (2014) 1212.
6. H. Zhekova, M. Krykunov, J. Autschbach, T. Ziegler, J. Chem. Theory Comput. 10 (2014) 3299.
7. M.E. Casida, in: D.P. Chong (Ed.), Recent Advances in Density-functional Methods, World Scientific, Singapore, 1995, p. 155.
8. A. D. Laurent, D. Jacquemin, Int. J. Quantum Chem. 113 (2013) 2019.
9. S. Grimme and F. Neese, J. Chem. Phys. 127 (2007) 154116.
10. D. Jacquemin, E. A. Perpète, G. Scalmani, M. J. Frisch, R. Kobayashi, C. Adamo, J. Chem. Phys. 126 (2007) 144105.

11. Y. Shao, M. Head-Gordon, A. I. Krylov, J. Chem. Phys. 118 (2003) 4807.

12. F. Wang, T. Ziegler, J. Chem. Phys. 121 (2004) 12191.

13. F. Wang, T. Ziegler, J. Chem. Phys. 122 (2005) 074109.

14. Z. Rinkevicius, H. Ågren, Chem. Phys. Lett. 491 (2010) 132.

15. Z. Rinkevicius, O. Vahtras, H. Ågren, J. Chem. Phys. 133 (2010) 114104.

16. Z. Li, W. Liu, J. Chem. Phys. 136 (2012) 024107.

17. Y. A. Bernard, Y. Shao, A. I. Krylov, J. Chem. Phys. 136 (2012) 204103.

18. M. Isegawa, D. G. Truhlar, J. Chem. Phys. 138 (2013) 134111.

19. X. Xu, K. R. Yang, D. G. Truhlar, J. Chem. Theory Comput. 10 (2014) 2070.

20. N. Minezawa and M. S. Gordon, J. Phys. Chem. A 113 (2009) 12749.

21. Y. Harabuchi, S. Maeda, T. Taketsugu, N. Minezawa, K. Morokuma, J. Chem. Theory Comput. 9 (2013) 4116.

22. X. Xu, S. Gozem, M. Olivucci, D. G. Truhlar, J. Chem. Phys. Lett. 4 (2012) 253.

23. P. Zhou, J. Liu, K. Han, G. He, J. Comput. Chem. 35 (2014) 109.

24. M. Filatov, M. Huix-Rotllant, J. Chem. Phys. 141 (2014) 024112.

25. M. W. Schmidt, K. K. Baldridge, J. A. Boatz, S. T. Elbert, M. S. Gordon, J. H. Jensen, S. Koseki, N. Matsunaga, K. A. Nguyen, S. J. Su, T. L. Windus, M. Dupuis, J. A.

Montgomery, Jr., J. Comput. Chem. 14 (1993) 1347.

26. M. S. Gordon, M.W. Schmidt, in: C. E. Dykstra, G. Frenking, K. S. Kim, G. E. Scuseria (Eds.), Theory and Applications of Computational Chemistry: The First Forty Years, Elsevier, Amsterdam, 2005, Chap. 41, pp. 1167–1189.
27. K. Yamaguchi, F. Jensen, A. Dorigo, K. N. Houk, Chem. Phys. Lett. 149 (1988) 537.
28. J. C. Slater, Phys. Rev. 81 (1951) 385.
29. S. H. Vosko, L. Wilk, M. Nusair, Can. J. Phys. 58 (1980) 1200.
30. A. D. Becke, Phys. Rev. A 38 (1988) 3098.
31. C. Lee, W. Yang, R. G. Parr, Phys. Rev. B37 (1988) 785.
32. A. D. Becke, J. Chem. Phys. 98 (1993) 5648.
33. P. J. Stephens, F. J. Devlin, C. F. Chablowski, M. J. Frisch, J. Phys. Chem. 98 (1994) 11623.
34. R. H. Hertwig, W. Koch, Chem. Phys. Lett. 268 (1997) 345.
35. J. P. Perdew, K. Burke, M. Ernzerhof, Phys. Rev. Lett. 77 (1996) 3865.
36. J. P. Perdew, K. Burke, M. Ernzerhof, Phys. Rev. Lett. 78 (1997) 1396.
37. C. Adamo, V. Barone, J. Chem. Phys. 110 (1999) 6158.
38. T. Yanai, D. P. Tew, N. C. Handy, Chem. Phys. Lett. 393 (2004) 51.

39. Y. Zhao, D. G. Truhlar, Theor. Chem. Acc. 120 (2008) 215.

40. Y. Zhao, D. G. Truhlar, J. Phys. Chem. A 110 (2006) 13126.

41. A. Schaefer, H. Horn, R. Ahlrichs, J. Chem. Phys. 97 (1992) 2571.

42. A. Schaefer, C. Huber, R. Ahlrichs, J. Chem. Phys. 100 (1994) 5829.

Vertical excitation energies of linear cyanine dyes: Non-collinear spin-flip time-dependent density functional theory

Noriyuki Minezawa

Fukui Institute for Fundamental Chemistry, Kyoto University,

Sakyo-ku, Kyoto 606-8103, Japan

E-mail: minezawa@fukui.kyoto-u.ac.jp

Appendix A. Supplementary data

Table S1. Basis set dependence of excitation energies for cyanine dyes.

Table S2. Excitation energies of CN5 at the SF-TDDFT/TZVP level.

Table S3. Excitation energies of CN7 at the SF-TDDFT/TZVP level.

Table S4. Excitation energies of CN9 at the SF-TDDFT/TZVP level.

Table S5. Excitation energies of CN11 at the SF-TDDFT/TZVP level.

Table S6. Excitation energies by the NSF2 method.

Table S7. Excitation energies by the SF2 method.

Table S1. Basis set dependence of excitation energies. Unit: eV.

Basis set	BHHLYP (collinear)			SVWN (non-collinear)		
	$\Omega(S_0 \mid T_1)$	$\Omega(S_1 \mid T_1)$	Total	$\Omega(S_0 \mid T_1)$	$\Omega(S_1 \mid T_1)$	Total
			CN5			
cc-pVDZ	−2.979	2.285	5.264	−3.439	0.543	3.982
TZVP	−2.961	2.218	5.178	−3.428	0.520	3.948
aug-cc-pVDZ	−2.954	2.204	5.158	−3.409	0.519	3.928
cc-pVTZ	−2.951	2.275	5.225	−3.421	0.541	3.962
TZVPP	−2.946	2.257	5.203	−3.416	0.535	3.951
aug-cc-pVTZ	−2.938	2.227	5.165	−3.402	0.529	3.931
			CN7			
cc-pVDZ	−2.116	1.941	4.057	−2.424	0.391	2.815
TZVP	−2.105	1.899	4.004	−2.418	0.379	2.797
aug-cc-pVDZ	−2.100	1.907	4.007	−2.409	0.381	2.790
cc-pVTZ	−2.093	1.949	4.042	−2.414	0.394	2.808

TZVPP	−2.090	1.941	4.031	−2.411	0.392	2.803
aug-cc-pVTZ	−2.086	1.927	4.013	−2.404	0.389	2.793
			CN9			
cc-pVDZ	−1.621	1.735	3.356	−1.871	0.308	2.179
TZVP	−1.613	1.706	3.319	−1.867	0.300	2.167
aug-cc-pVDZ	−1.608	1.721	3.329	−1.862	0.303	2.165
cc-pVTZ	−1.601	1.751	3.356	−1.864	0.312	2.176
TZVPP	−1.598	1.746	3.344	−1.862	0.311	2.173
aug-cc-pVTZ	−1.595	1.739	3.334	−1.857	0.309	2.166
			CN11			
cc-pVDZ	−1.304	1.592	2.896	−1.525	0.255	1.780
TZVP	−1.297	1.570	2.867	−1.523	0.250	1.773
aug-cc-pVDZ	−1.293	1.589	2.882	−1.520	0.253	1.773
cc-pVTZ	−1.286	1.612	2.898	−1.520	0.260	1.780
TZVPP	−1.284	1.609	2.893	−1.519	0.259	1.778
aug-cc-pVTZ	−1.281	1.606	2.887	−1.516	0.258	1.774

Table S2. Vertical excitation energies of CN5 at the SF-TDDFT/TZVP level.[a]

Functional	E(ref.) / a.u.	$\langle S^2 \rangle$	$E(^1A_1)$ / a.u.	$\langle S^2 \rangle$	$E(^1B_2)$ / a.u.	$\langle S^2 \rangle$
BLYP	−227.68383	2.004	N/A			
			−227.80213	0.008	−227.66060	0.019
			−227.79893	0.007	−227.65436	0.013
			−227.79806	0.006	−227.65296	0.012
B3LYP	−227.63487	2.006	−227.74208	0.009	−227.57290	0.025
			−227.75294	0.010	−227.59306	0.049
			−227.75041	0.009	−227.58768	0.040
			−227.74963	0.009	−227.58623	0.038
BHHLYP	−227.62754	2.012	−227.73634	0.021	−227.54604	0.090
			−227.74258	0.020	−227.55324	0.341
			−227.74035	0.021	−227.55335	0.103
			−227.73917	0.021	−227.55053	0.099
CAMB3LYP	−227.64755	2.007	−227.75786	0.016	−227.56632	0.051
			−227.76810	0.013	−227.58567	0.097

			−227.76595	0.013	−227.58203	0.075
			−227.76485	0.013	−227.57948	0.071
M06	−227.59685	2.007	−227.70989	0.011	−227.53927	0.035
			N/A			
			−227.73840	0.029	−227.59228	0.125
			−227.71340	0.020	−227.55075	0.056
M06-2X	−227.64892	2.009	−227.78329	0.018	−227.59746	0.112
			N/A			
			−227.79117	0.019	−227.61221	0.136
			−227.77297	0.023	−227.57961	0.072
M06-HF	−227.67544	2.014	−227.85571	0.035	−227.66191	0.269
			N/A			
			−227.81735	0.044	−227.57970	0.154
			−227.80600	0.129	−227.57625	0.115
PBE	−227.48324	2.003	N/A			
			−227.60065	0.010	−227.45911	0.020

			−227.59749	0.007	−227.45234	0.013
			−227.59852	0.008	−227.45445	0.015
PBE0	−227.49884	2.007	−227.60374	0.010	−227.42939	0.035
			−227.61602	0.028	−227.45073	0.060
			−227.61203	0.011	−227.44442	0.050
			−227.61326	0.011	−227.44705	0.053
PBE50	−227.52168	2.012	−227.62792	0.020	−227.43619	0.086
			−227.63543	0.020	−227.45176	0.115
			−227.63270	0.019	−227.44529	0.101
			−227.63407	0.019	−227.44835	0.106
SVWN	−225.77825	2.002	N/A			
			−225.90424	0.005	−225.75914	0.012
			−225.90424	0.005	−225.75914	0.012
			−225.90424	0.005	−225.75914	0.012

aEach block has four rows: collinear and non-collinear (NCOL0, NCOL1, NCOL2) calculations from top to bottom.

Table S3. Vertical excitation energies of CN7 at the SF-TDDFT/TZVP level.[a]

Functional	E(ref.) / a.u.	$\langle S^2 \rangle$	$E(^1A_1)$ / a.u.	$\langle S^2 \rangle$	$E(^1B_2)$ / a.u.	$\langle S^2 \rangle$
BLYP	−305.12338	2.003	N/A			
			−305.20685	0.006	−305.10638	0.020
			−305.20438	0.004	−305.10192	0.017
			−305.20376	0.004	−305.10098	0.017
B3LYP	−305.05806	2.005	−305.13399	0.011	−305.00875	0.030
			−305.14203	0.008	−305.02347	0.062
			−305.14009	0.008	−305.01975	0.052
			−305.13954	0.008	−305.01878	0.049
BHHLYP	−305.04832	2.011	−305.12566	0.031	−304.97853	0.127
			−305.13031	0.026	−304.98825	0.158
			−305.12855	0.028	−304.98444	0.145
			−305.12770	0.029	−304.98276	0.142
CAMB3LYP	−305.07161	2.007	−305.14991	0.032	−304.99887	0.086
			−305.15743	0.022	−305.01432	0.137

			−305.15586	0.024	−305.01110	0.120
			−305.15506	0.025	−305.00950	0.115
M06	−305.00622	2.006	−305.08549	0.011	−304.95799	0.041
			N/A			
			−305.10654	0.019	−304.99849	0.161
			−305.08744	0.010	−304.97758	0.966
M06-2X	−305.08452	2.007	−305.18468	0.026	−305.04035	0.148
			N/A			
			−305.19010	0.022	−305.05195	0.188
			−305.17657	0.038	−305.02269	0.093
M06-HF	−305.12476	2.013	−305.26109	0.052	−305.10609	0.412
			N/A			
			−305.23261	0.098	−305.04086	0.204
			−305.23053	0.123	−305.02882	0.179
PBE	−304.85431	2.003	N/A			
			−304.93735	0.006	−304.83614	0.020

			−304.93475	0.004	−304.83176	0.014
			−304.93564	0.005	−304.83338	0.017
PBE0	−304.87523	2.006	−304.94978	0.013	−304.81960	0.039
			−304.95838	0.010	−304.83502	0.078
			−304.95580	0.010	−304.83068	0.065
			−304.95680	0.010	−304.83267	0.070
PBE50	−304.90623	2.010	−304.98203	0.029	−304.83383	0.123
			−304.98763	0.025	−304.84513	0.158
			−304.98548	0.026	−304.84080	0.144
			−304.98662	0.026	−304.84308	0.152
SVWN	−302.53870	2.002	N/A			
			−302.62758	0.004	−302.52478	0.012
			−302.62758	0.004	−302.52478	0.012
			−302.62758	0.004	−302.52478	0.012

[a]Each block has four rows: collinear and non-collinear (NCOL0, NCOL1, NCOL2) calculations from top to bottom.

Table S4. Vertical excitation energies of CN9 at the SF-TDDFT/TZVP level.[a]

Functional	E(ref.) / a.u.	$\langle S^2 \rangle$	$E(^1A_1)$ / a.u.	$\langle S^2 \rangle$	$E(^1B_2)$ / a.u.	$\langle S^2 \rangle$
BLYP	−382.54529	2.002	N/A			
			−382.60972	0.005	−382.53168	0.020
			−382.60770	0.004	−382.52823	0.023
			−382.60722	0.004	−382.52749	0.025
B3LYP	−382.46384	2.006	−382.52237	0.014	−382.42182	0.044
			−382.52879	0.010	−382.43407	0.074
			−382.52726	0.011	−382.43082	0.063
			−382.52682	0.011	−382.43001	0.061
BHHLYP	−382.45218	2.016	−382.51144	0.049	−382.38950	0.161
			−382.51516	0.044	−382.39778	0.199
			−382.51376	0.046	−382.39457	0.181
			−382.51299	0.047	−382.39295	0.174
CAMB3LYP	−382.47822	2.012	−382.53819	0.054	−382.41090	0.123
			−382.54421	0.041	−382.42400	0.171

			−382.54304	0.044	−382.42135	0.161
			−382.54238	0.046	−382.41988	0.155
M06	−382.39769	2.007	−382.45807	0.015	−382.35485	0.056
			N/A			
			−382.47501	0.019	−382.38886	0.188
			−382.45881	0.015	−382.36321	0.086
M06-2X	−382.50284	2.012	−382.58199	0.044	−382.46207	0.184
			N/A			
			−382.58625	0.039	−382.47201	0.229
			−382.57499	0.249	−382.44678	0.124
M06-HF	−382.55668	2.026	−382.66690	0.098	−382.53558	0.499
			N/A			
			−382.64305	0.150	−382.47789	0.267
			−382.64516	0.214	−382.46861	0.906
PBE	−382.20779	2.002	N/A			
			−382.27189	0.005	−382.19317	0.024

			−382.26970	0.004	−382.18983	0.020
			−382.27046	0.004	−382.19120	0.022
PBE0	−382.23441	2.007	−382.29177	0.019	−382.18664	0.055
			−382.29864	0.013	−382.20013	0.101
			−382.29660	0.015	−382.19575	0.080
			−382.29747	0.014	−382.19728	0.085
PBE50	−382.27402	2.016	−382.33197	0.049	−382.20925	0.158
			−382.33643	0.042	−382.21868	0.194
			−382.33474	0.045	−382.21517	0.181
			−382.33572	0.044	−382.21702	0.188
SVWN	−379.28099	2.001	N/A			
			−379.34961	0.003	−379.26995	0.012
			−379.34961	0.003	−379.26995	0.012
			−379.34961	0.003	−379.26995	0.012

[a]Each block has four rows: collinear and non-collinear (NCOL0, NCOL1, NCOL2) calculations from top to bottom.

Table S5. Vertical excitation energies of CN11 at the SF-TDDFT/TZVP level.[a]

Functional	E(ref.) / a.u.	$\langle S^2 \rangle$	$E(^1A_1)$ / a.u.	$\langle S^2 \rangle$	$E(^1B_2)$ / a.u.	$\langle S^2 \rangle$
BLYP	−459.95915	2.002	N/A			
			−460.01165	0.005	−459.94777	0.022
			−460.00995	0.004	−459.94488	0.032
			−460.00954	0.003	−459.94424	0.035
B3LYP	−459.86158	2.007	−459.90916	0.019	−459.82446	0.061
			−459.91467	0.016	−459.83460	0.085
			−459.91328	0.015	−459.83219	0.076
			−459.91292	0.015	−459.83150	0.074
BHHLYP	−459.84798	2.023	−459.89565	0.073	−459.79028	0.201
			−459.89888	0.065	−459.79736	0.233
			−459.89763	0.068	−459.79480	0.222
			−459.89701	0.070	−459.79335	0.215
CAMB3LYP	−459.87661	2.018	−459.92490	0.082	−459.81334	0.164
			−459.93023	0.067	−459.82499	0.215

			−459.92906	0.070	−459.82263	0.205
			−459.92847	0.071	−459.82128	0.198
M06	−459.78091	2.009	−459.82948	0.021	−459.74198	0.076
			N/A			
			−459.84391	0.021	−459.77176	0.214
			−459.83168	0.027	−459.75176	0.167
M06-2X	−459.91259	2.016	−459.97807	0.065	−459.87437	0.220
			N/A			
			−459.98166	0.058	−459.88320	0.271
			−459.97130	0.078	−459.85806	0.142
M06-HF	−459.97930	2.037	−460.07194	0.145	−459.95632	0.588
			N/A			
			−460.05090	0.210	−459.90378	0.332
			−460.04961	0.273	−459.87973	0.542
PBE	−459.55323	2.002	N/A			
			−459.60545	0.005	−459.54041	0.089

			−459.60358	0.004	−459.53819	0.028
			−459.60357	0.037	−459.53887	0.026
PBE0	−459.58559	2.009	−459.63213	0.026	−459.54313	0.075
			−459.63869	0.026	−459.55565	0.125
			−459.63619	0.021	−459.55100	0.097
			−459.63694	0.020	−459.55239	0.103
PBE50	−459.63377	2.023	−459.68032	0.073	−459.57432	0.200
			−459.68435	0.065	−459.58276	0.238
			−459.68268	0.068	−459.57957	0.223
			−459.68353	0.067	−459.58120	0.231
SVWN	−456.01503	2.001	N/A			
			−456.07099	0.003	−456.00583	0.012
			−456.07099	0.003	−456.00583	0.012
			−456.07099	0.003	−456.00583	0.012

[a]Each block has four rows: collinear and non-collinear (NCOL0, NCOL1, NCOL2) calculations from top to bottom.

Table S6. Excitation energies by the NSF2 method.[a] Unit: eV.

Functional	CN5	CN7	CN9	CN11	MSE[b]
BLYP	N/A				
	3.81	2.71	2.11	1.73	−1.05
	3.98	2.83	2.20	1.81	−0.94
	4.01	2.86	2.22	1.83	−0.91
B3LYP	4.85	3.59	2.88	2.42	**−0.21**
	4.31	3.19	2.54	2.15	−0.60
	4.45	3.29	2.63	2.21	−0.50
	4.49	3.31	2.65	2.23	−0.47
BHHLYP	5.36	4.13	3.42	2.95	0.32
	5.17	3.87	3.19	2.76	**0.10**
	5.16	3.97	3.28	2.83	**0.17**
	5.24	4.01	3.32	2.87	**0.22**
CAMB3LYP	5.38	4.22	3.55	3.11	0.42

	4.86	3.80	3.19	2.79	**0.02**
	4.96	3.89	3.27	2.86	**0.10**
	5.03	3.93	3.31	2.89	**0.15**
M06	4.77	3.56	2.90	2.46	**−0.22**
	N/A				
	3.32	2.46	1.97	1.65	−1.29
	4.45	3.03	2.67	2.20	−0.55
M06-2X	4.76	3.61	2.96	2.54	**−0.17**
	N/A				
	4.36	3.29	2.69	2.30	−0.48
	5.25	4.09	3.38	2.99	**0.28**
M06-HF	3.93	3.06	2.53	2.20	−0.71
	N/A				
	6.17	4.84	4.10	3.63	1.04
	6.26	5.17	4.35	4.28	1.37
PBE	N/A				

	3.82	2.73	2.13	1.76	−1.03
	4.01	2.85	2.22	1.82	−0.92
	3.95	2.81	2.18	1.80	−0.96
PBE0	5.03	3.74	3.01	2.55	**−0.06**
	4.45	3.32	2.65	2.21	−0.49
	4.62	3.44	2.76	2.33	−0.35
	4.55	3.38	2.72	2.29	−0.41
PBE50	5.45	4.18	3.45	2.98	0.37
	5.02	3.87	3.20	2.75	**0.07**
	5.20	3.99	3.29	2.84	**0.19**
	5.12	3.93	3.24	2.79	**0.13**
SVWN	N/A				
	3.82	2.72	2.11	1.73	−1.04
	3.82	2.72	2.11	1.73	−1.04
	3.82	2.72	2.11	1.73	−1.04

[a]Each block has four rows: collinear and non-collinear (NCOL0, NCOL1, NCOL2) calculations from top to bottom.

[b]Mean signed error. Reference is the DMC excitation energies: 5.03, 3.83, 3.09, and 2.62 eV.

Table S7. Excitation energies by the SF2 method.[a] Unit: eV.

Functional	CN5	CN7	CN9	CN11	MSE[b]
BLYP	N/A				
	3.81	2.71	2.11	1.73	−1.05
	3.98	2.83	2.21	1.81	−0.94
	4.01	2.86	2.23	1.83	−0.91
B3LYP	4.86	3.59	2.88	2.42	**−0.21**
	4.31	3.19	2.55	2.15	−0.59
	4.46	3.29	2.64	2.22	−0.49
	4.49	3.32	2.66	2.23	−0.47
BHHLYP	5.37	4.14	3.43	2.96	0.33
	5.20	3.88	3.20	2.77	**0.12**
	5.17	3.98	3.29	2.84	**0.18**
	5.25	4.02	3.33	2.88	**0.23**
CAMB3LYP	5.39	4.23	3.56	3.12	0.43

	4.87	3.81	3.20	2.80	**0.03**
	4.96	3.90	3.28	2.87	**0.11**
	5.03	3.94	3.32	2.90	**0.16**
M06	4.77	3.57	2.90	2.47	**−0.22**
	N/A				
	3.33	2.47	1.98	1.66	−1.28
	4.46	3.13	2.67	2.21	−0.53
M06-2X	4.77	3.62	2.97	2.56	**−0.16**
	N/A				
	4.37	3.30	2.70	2.32	−0.47
	5.25	4.09	3.38	3.00	**0.29**
M06-HF	3.96	3.10	2.57	2.24	−0.67
	N/A				
	6.19	4.86	4.12	3.65	1.06
	6.28	5.19	4.49	4.34	1.43
PBE	N/A				

	3.82	2.74	2.13	1.77	−1.03
	4.01	2.85	2.22	1.82	−0.92
	3.95	2.81	2.18	1.81	−0.96
PBE0	5.03	3.74	3.01	2.55	**−0.06**
	4.45	3.32	2.65	2.21	−0.48
	4.63	3.44	2.77	2.34	−0.35
	4.55	3.39	2.73	2.30	−0.40
PBE50	5.45	4.19	3.46	2.99	0.38
	5.03	3.88	3.21	2.76	**0.08**
	5.21	4.00	3.30	2.85	**0.20**
	5.13	3.94	3.25	2.80	**0.14**
SVWN	N/A				
	3.82	2.72	2.11	1.73	−1.04
	3.82	2.72	2.11	1.73	−1.04
	3.82	2.72	2.11	1.73	−1.04

[a]Each block has four rows: collinear and non-collinear (NCOL0, NCOL1, NCOL2) calculations from top to bottom.

[b]Mean signed error. Reference is the DMC excitation energies: 5.03, 3.83, 3.09, and 2.62 eV.